LWT - Food Science and Technology 214 (2024) 117142

Contents lists available at ScienceDirect

LWT

journal homepage: www.elsevier.com/locate/lwt

Preparation of wheat germ albumin polypeptide microcapsules embedded with starch sodium octenylsuccinate/sodium alginate-based materials and sustained-release properties *in vitro*

Shuangqi Tian [a,b,*], Yuqiu Hu [a,b], Ke Du [a], Jing Lu [c]

[a] College of Food Science and Technology, Henan University of Technology, Zhengzhou, 450001, China
[b] Food Laboratory of Zhongyuan, Luohe, 462300, China
[c] Department of Molecular Sciences, Swedish University of Agricultural Sciences, PO Box 7015, SE-75007, Uppsala, Sweden

ARTICLE INFO

Keywords:
Microcapsules
Wheat germ albumin
Polypeptide
Sustained release properties

ABSTRACT

The enzymatic hydrolysis products of wheat germ albumin have been extensively studied due to their strong antioxidant properties. The small intestine is an important part for absorbing active substances, but polypeptides are not acid-resistant and are easily hydrolyzed and lose their activity in the stomach, which does not achieve the effect of small intestine absorption. In this study, the optimal process conditions for microencapsulation of wheat germ albumin polypeptides were determined based on response surface optimization experiments as follows: wall to material ratio (starch sodium octenylsuccinate (SSOS): sodium alginate (SA) = 3:1), homogenization time 10 min, and wall to core ratio 20:1. The embedding rate of microcapsules prepared under these conditions was 65.33%. The average particle size of microcapsules was 100.21 μm. SEM results showed that the freeze-drying microcapsules had a sheet-like structure. The increased intensity of the amide A band in the microcapsules in Fourier transform infrared (FT-IR) spectroscopy indicated the formation of hydrogen bonds between the wall materials, while thermogravimetric analysis confirmed the protective effect of microcapsules on the formation of wheat germ albumin polypeptides. The release rates of microcapsules in gastric and intestinal juice were 26.54% and 84.41%, respectively, indicating that microcapsules had a sustained release effect.

1. Introduction

Wheat is one of the three largest grains in the world, and also the most important food crop for human beings (Kettlewell, Byrne, & Jeffery, 2023). Wheat products account for a large proportion of the world's population's diet (Ji et al., 2024). Wheat germ is the key to the growth and development of wheat and the source of wheat life. However, in the process of wheat production and processing, wheat germ is the byproduct of wheat processing, accounting for 2%–3% of wheat grains, in the process of wheat production and processing is often ignored (Brestenský, Nitrayová, Patráš, & Heger, 2013; Olalere & Gan, 2023). In the process of wheat milling, the addition of wheat germ will not only affect the color of flour but also affect the shelf life of flour (Cuomo et al., 2024; Giménez et al., 2013). Wheat germ has been separated and mixed into wheat bran in the process of making wheat flour for a long time, which resulted in the waste of rich nutrients and active functional components in wheat germ (Liu et al., 2021; Zhuang et al., 2022).

Protein is an important component of wheat germ, which can be divided into albumin, globulin, gliadin and glutenin (Liu et al., 2024; Zhang et al., 2024). The content of total protein in wheat germ is as high as 30%, which is the highest component in wheat germ (Gao et al., 2023). The protein in wheat germ mainly includes four kinds of protein, among which albumin, globulin, glutenin, and gliadin accountes for 30.2%, 18.9%, 0.3%–0.37%, and 14.0%, respectively (Abarghoei, Goli, & Shahi, 2023). Wheat germ protein is a complete protein with a reasonable essential amino acid composition (Wang et al., 2019). It contains eight essential amino acids, of which 1.9% are methionine and 2.5% are histidine, the content of the first limiting amino acid-lysine is much higher than that of rice and flour (Zhu, Zhou, & Qian, 2006). Compared with wheat germ protein, wheat germ globulin and wheat germ glutenin, the solubility of wheat germ albumin powder is the best (Tian, Du, Yan, & Li, 2022). The good or bad solubility of a protein often determines its availability in food and drug industry. The good solubility of wheat germ albumin makes the application of wheat germ in product

* Corresponding author. College of Food Science and Technology, Henan University of Technology, Zhengzhou, 450001, China.
E-mail address: tianshuangqi@haut.edu.cn (S. Tian).

https://doi.org/10.1016/j.lwt.2024.117142
Received 28 October 2024; Received in revised form 29 November 2024; Accepted 30 November 2024
Available online 2 December 2024

development more possible (Liu, Chen, Wang, & Wang, 2013; Tian et al., 2022). Among the proteins contained in wheat germ, albumin has better nutritional value and higher amino acid score than other proteins (Brandolini & Hidalgo, 2012; Zhang et al., 2024).

Bioactive peptides can not only regulate the metabolic function and physiological activities of the human body, but also enhance immunity, regulate hormones, inhibit bacteria, resist viruses, lower blood pressure and blood lipids (Bizzotto et al., 2024; Tonolo et al., 2025). Bioactive peptides are easier to digest and absorb than proteins, providing new ideas for the application of wheat germ protein (Karami, Peighambardoust, Hesari, Akbari-Adergani, & Andreu, 2019; Zhang et al., 2023). Bioactive peptides can be obtained from protein precursors by digestive enzymes during food processing or storage processes such as ripening, fermentation, and cooking, and can also be hydrolyzed *in vitro* by proteolytic enzymes (Guo, Chen, & Chen, 2023; Mao et al., 2024). Enzymatic hydrolysis or microbial fermentation of defatted wheat germ protein can yield bioactive peptides from wheat germ (Hosseini et al., 2022). The enzymatic hydrolysis products of wheat germ albumin have been extensively studied in the field of functional food development due to their strong antioxidant properties (Karami et al., 2019; Liu et al., 2013; Tian et al., 2022). The small intestine is an important site for absorbing active substances. Protein and peptide functional factors cannot simply diffuse through the intercellular space and are difficult to fuse with the cell membrane. Without the help of carriers, it is difficult to enter the bloodstream through the small intestine mucosa (Plaisancié et al., 2013; Wu et al., 2024). Sodium alginate (SA) has been widely studied as a wall material mainly due to its biocompatibility and embedding characteristics, and starch sodium octenylsuccinate (SSOS) has dual effects of emulsification and thickening (Wang et al., 2017). However, few research has focused on the use of starch based microcapsules for the sustained release of bioactive peptides. In this study, using the encapsulation rate of microcapsules as an evaluation index, the process conditions for microencapsulation of wheat germ albumin polypeptides were optimized based on single factor experiments and Box Behnken response surface analysis by freeze-drying method. The microcapsules were characterized using methods such as particle size analysis, electron microscopy scanning (SEM), fourier transform infrared (FT-IR) spectroscopy, and thermogravimetric analysis (TGA), and the sustained-release properties of wheat germ albumin polypeptide microcapsules were studied through simulated gastric and intestinal digestion experiments.

2. Materials and methods

2.1. Materials

Wheat germ albumin polypeptides with a molecular weight less than 3 kDa were prepared by the laboratory itself (Tian, Meng, Du, & Chen, 2023). To separate the hydrolysate of wheat germ albumin, the ultrafiltration method was used, and polypeptides with molecular weights greater than 3 kDa and less than 3 kDa were isolated. SSOS (Octenyl succinic acid group 3%) was purchased from Zhengzhou Chaofan Chemical Co., Ltd (Henan, China). Sodium alginate (SA) (CAS 9005-38-3, purity of 99% viscosity (2% g/100 mL at 25 °C): 2.000 cps), batch No QN0701 with weight-average molecular weight (Mw) of 198 kDa was purchased from Boaolaibo Technology Co., Ltd (Beijing, China). Pepsin (3000 NFU/g) and trypsin (250 U/mg) were purchased from Solaibao Technology Co., Ltd (Beijing, China). All other reagents were analytical grade.

2.2. Preparation of microcapsules

The wall material consisted of SSOS and SA. Distilled water was used to prepare different concentrations of starch sodium octenylsuccinate (SSOS) and sodium alginate (SA), respectively. The solutions were thoroughly stirred and dissolved in a constant temperature water bath, and left to stand with an exhaust bubble for later use. Microcapsules were prepared according to the method by Li et al. (Li, Shin, Lee, Chen, & Park, 2016) with some modifications. Wheat germ albumin polypeptides were dissolved in anhydrous ethanol and filtered through a 0.4 μ m filter to remove undissolved crystals. The wall material (SSOS-SA) was dissolved in distilled water and subjected to ultrasonic treatment to stabilize its system distribution. Wheat germ albumin polypeptide ethanol solution was slowly drip into SSOS-SA solution during homogenization process to prepare SSOS-SA wheat germ albumin polypeptide composite samples. The samples were heated appropriately to remove ethanol, and after ultrasonic treatment, dried with a freeze dryer (Model 7753031, Labconco Corporation, USA) (vacuum degree of 7 Pa, vacuum pumping for 18 h, continuous drying time of about 30 h) to obtain microcapsules, which was stored at −20 °C for use.

2.3. Experimental design and model validation

The process parameters (wall material ratio, homogenization time, and wall to core ratio) were used as independent variables, which affected microcapsule embedding rate. The effects of wall material ratio (SSOS:SA = 1:1–6:1), homogenization time (30–70 °C), and wall to core ratio (5:1–30:1) on microcapsule embedding rate through single factor experiments. Therefore, Box-Behnken design-response surface methodology (BBD-RSM) was used to obtain the optimal microcapsule embedding rate and determine the correlation between the microcapsule embedding variables. The optimal microcapsule embedding rate was obtained using Design Expert 8.0.6 software. The experiment was conducted under optimal conditions to obtain experimental data that was compared to the predicted values of the model.

2.4. Determination of microcapsule embedding rate

Microcapsules embedding rate was determined according to the method by Xiao et al. (Xiao et al., 2023) with some modifications. 0.5 g of microcapsules were taken into a centrifuge tube, and added 10 mL distilled water. The mixed solution was centrifuged at 4000×*g* for 10 min. 1 mL of the supernatant was taken and added 5 mL Coomassie Brilliant Blue. Its absorbance at 595 nm was measured. Microcapsule embedding rate was evaluated as fellow (1):

$$\text{Embedding rate } (\%) = \left(\frac{C_1}{C_0}\right) \times 100 \quad (1)$$

where C_0 represents the absorbance value of wheat germ albumin polypeptide content added to the solution, C_1 represents the absorbance value of wheat germ albumin polypeptide content inside microcapsules.

2.5. Particle size analysis

The freeze-drying microcapsule samples were passed through an 80 mesh sieve. A small amount of sample was taken and placed it in the sample slot of the fully automatic laser particle size analyzer (winner2000ZDE, Jinan Micro Nano Particle Instrument Co., Ltd, Shandong, China) to evenly disperse the sample at the inlet, ensuring that the refractive index of the scanning result reached 8–15% before collecting data.

2.6. Scanning electron microscopy (SEM)

Scanning electron microscope (SEM, SU8000; Hitachi, Japan) was used to observe the morphology of different samples. The samples were coated with conductive adhesive on the copper plate and then stored in a vapor deposition chamber for gold plating. The microstructures of different samples were observed using SEM with a magnification of 500 times at an accelerating voltage of 300 kV.

2.7. Fourier transform infrared (FT-IR) spectroscopy

The Fourier transform infrared spectrometer (WQF-510, Beifen Raleigh Analytical Instrument Co., Ltd, Beijing, China) was used to record FT-IR spectra. The samples passed through a 100 meshes sieve. In order to study the main binding sites of different samples, 1 mg of the sample was weighed into a quartz mortar, and added 0.4 g potassium bromide (dried to constant weight). The mixed sample was ground evenly. 0.1 g of ground sample was taken, and a tablet was used to press the sample into a transparent sheet. The sample was scanned 32 times in the frequency range of 4000-400 cm^{-1} with at a resolution of 4 cm^{-1}, and analyzed the peak signal in the spectrum using Omnic software (Thermo Nicolet Co., Madison, WI, USA).

2.8. Thermogravimetry-derivative thermogravimetry (TG-DTG) analysis

The thermal stability of different samples was measured using a thermogravimetric analyzer (Q50, TA Instruments, USA), including thermogravimetry-derivative thermogravimetry (TG-DTG). 6 mg sodium octenyl succinate starch, sodium alginate, peptides under 3 kDa and microcapsules were taken separately, and placed them in a small crucible. The conditions of thermogravimetric analysis were as follows: N_2 flow rate 20 mL/min, temperature 50–500 °C, heating rate 10 °C/min.

2.9. Sustained-release experiment of wheat germ polypeptide microcapsules in vitro

5 g wheat germ polypeptide microcapsules were dissolved in 100 mL of artificial simulated gastric juice and intestinal juice respectively. The artificial simulated gastric juice was prepared according to the method by Zheng et al. with some modifications. 7.0 mL hydrochloric acid was taken in a beaker, and added 600 mL distilled water to dissolve. Then, 10 g pepsin was dissolved in the hydrochloric acid solution, and the acidic pepsin solution was finally diluted to 1 L with distilled water, which was the artificial simulated gastric juice (Zheng, Choi, Seong, & Chung, 2020). The artificial simulated intestinal juice was prepared according to the method by Zheng et al. with some modifications. 6.8 g potassium dihydrogen phosphate was weighed and dissolved it in 600 mL distilled water. The dissolved solution was adjusted the pH to 6.8 with 1 mol/L NaOH solution. 10 g trypsin was weighed and dissolved it in potassium dihydrogen phosphate solution. After the complete dissolution of trypsin, the trypsin solution was diluted to 1 L with distilled water to obtain artificial simulated intestinal juice (Zheng et al., 2020). Sustained-release experiment of wheat germ polypeptide microcapsules *in vitro* was placed in a constant temperature water bath. The shaking speed was adjusted to 150 rpm and the temperature to 37 °C. 2 mL sample solution was taken at intervals, and measured the release rate of wheat germ polypeptide microcapsules in simulated digestive juice (Zheng et al., 2020).

2.10. Statistical analysis

SPSS 16.0 software was used to perform a significant analysis of the data at the $P < 0.05$ detection level. One-way ANOVA (analysis of variance) was performed to evaluate significant differences, verified with Tukey's HSD (honestly significant difference) test. Origin 2018 was selected to plot the experimental data, and the average of three parallel experiment results was taken as the data.

3. Results and discussion

3.1. Effect of different factors on the microcapsule embedding rate

Under the conditions of a wall to core ratio of 20:1 and a homogenization time of 7.5 min, the effect of different ratios of SSOS and SA on the microcapsule embedding rate was studied. The results were shown in Fig. 1a. When the wall material ratio SSOS: SA = 3:1, the microcapsule embedding rate reached its maximum value of 63.73%. When the wall material ratio was greater than 3:1, the microcapsule embedding rate showed a significant increasing trend with the increase of the relative content of wall material ratio SA. However, when the wall material ratio was less than 3:1, the microcapsule embedding rate no longer changed significantly with the increase in the relative amount of SA. Perhaps due to SSOS being a wall material with high hydrophilicity and oleophilicity, when the content of sodium alginate was low, the flowability of the wall material was high, making it difficult to form a uniform emulsion with wheat germ peptides, resulting in a lower microcapsule embedding rate (Lai et al., 2021). However, as the content of sodium alginate increased, the viscosity of the wall material also increased, making it easier for the wall and core materials to achieve the purpose of embedding during homogenization (Jiang, Zhou, Wang, Xue, & Niu, 2021).

Under the conditions of a wall to core ratio of 20:1 and a wall to material ratio of SSOS: SA = 1:1, the effect of changing homogenization time on microcapsule embedding rate was explored, and the results were shown in Fig. 1b. As shown in Fig. 1b, with the prolongation of homogenization time, the microcapsule embedding rate showed a significant phenomenon of first increasing and then slowly decreasing ($P < 0.05$). When the homogenization time reached 7.5 min, the microcapsule embedding rate obtained its maximum value of 63.08%. When the homogenization time was short, the wall material and core material did not reach sufficient contact, while when the homogenization time was too long, it would reduce the stability of the microcapsule solution, leading to the phenomenon of layering in the solution, reducing the degree of bonding between the wall material and core material, and thus reducing the microcapsule embedding rate (Do et al., 2024).

Under the conditions of homogenization time of 5 min and wall to core ratio of SSOS: SA = 1:1, the effect of different wall to core ratios on the microcapsule embedding rate was studied. The results were shown in Fig. 1c. As the proportion of wall materials increased, the embedding rate of microcapsules also showed a trend of first increasing and then decreasing ($P < 0.05$). When the wall to core ratio was 20:1, the embedding rate of microcapsules reached its maximum value of 51.93%. Perhaps due to the relatively high content of wheat germ peptides when the wall material content was low, the wall material in the solution was not sufficient to effectively encapsulate the peptides. As the wall material content increased, wheat germ peptides were more easily encapsulated by the wall material. If the wall material content was too high, it would lead to incomplete utilization of the wall material, resulting in a decrease in the embedding rate (Xun et al., 2023).

3.2. Optimization of microcapsule embedding rate

Based on a single factor experiment, a three factor three-level response surface optimization experiment was designed with wall to core ratio (X_1), homogenization time (X_2), and wall to core ratio (X_3) as influencing factors, and microcapsule embedding rate (Y) as the evaluation index, and a three factor three-level RSM optimization experiment was designed. RSM with BBD was performed to optimum microcapsule embedding condition for the embedding rate (Table 1). According to BBD experimental principles, Table 2 provide the design factors, levels, and results of the response surface experiment.

By fixing three independent variables and changing the remaining variables of each response, a response surface graph was formed. Regression fitting was performed on the data in Table 1 using Design Expert 8.0.6 software to obtain a linear regression equation for the microcapsule embedding rate. Perform regression fitting on the data to obtain a quadratic regression equation:

$$Y = 64.20\text{-}1.09X_1 + 0.82X_2 \text{-} 1.92X_3 + 0.22X_1X_2 \text{-} 1.41X_1X_3 \text{-} 0.34X_2X_3 \text{-} 4.33 \times {}^{2}_{1} + 0.064X_2^2 \text{-} 6.96 \times {}^{2}_{3} \quad (2)$$

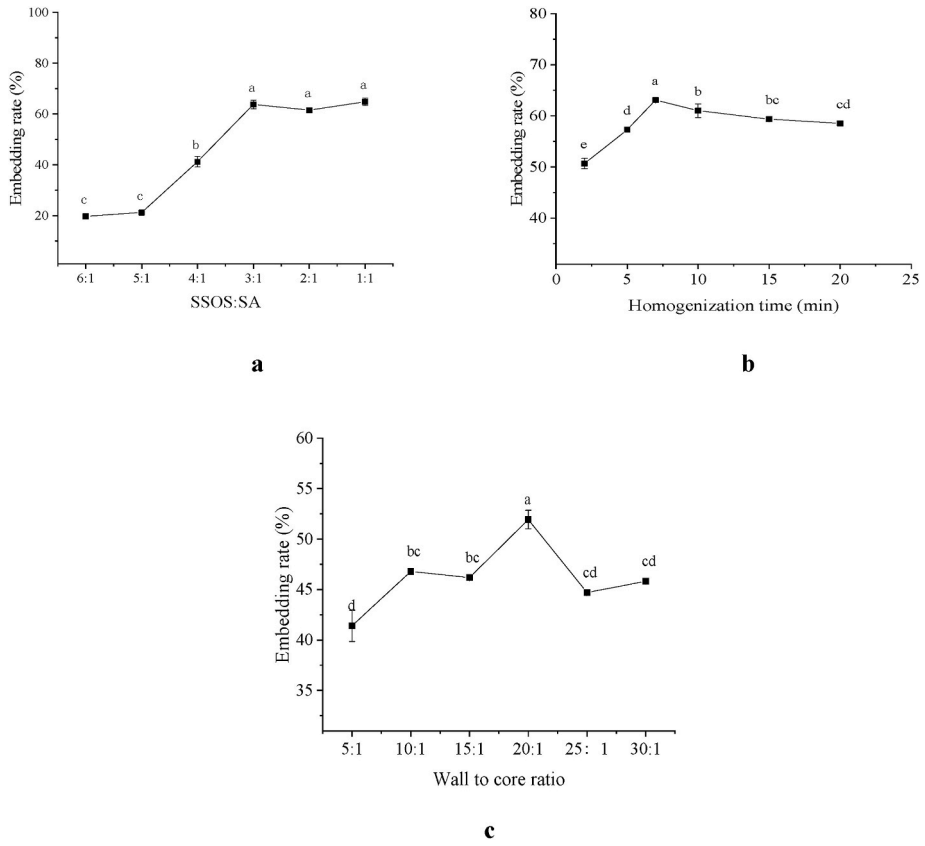

Fig. 1. The effect of different factors on the microcapsule embedding rate (a: SSOS:SA; b: Homogenization time; c: Wall to core ration).

Table 1
The results based on response surface experimental design.

Run	Wall to core ratio (X_1)	Homogenization time (min, X_2)	Wall to core ratio(X_3)	Embedding rate(%)
1	25:1	7.5	4:1	48.18
2	15:1	10	3:1	62.01
3	20:1	7.5	3:1	63.48
4	25:1	5	3:1	57.42
5	20:1	10	4:1	55.96
6	20:1	7.5	3:1	63.48
7	15:1	7.5	4:1	52.92
8	20:1	7.5	3:1	64.16
9	25:1	10	3:1	60.03
10	20:1	7.5	3:1	64.38
11	15:1	7.5	2:1	54.83
12	20:1	7.5	3:1	64.61
13	20:1	5	2:1	57.98
14	15:1	5	3:1	60.29
15	20:1	5	4:1	55.51
16	25:1	7.5	2:1	55.73
17	20:1	10	2:1	59.78

Table 2
The quadratic model analysis of RSM.

Factors	Sum of squares squares	df	Mean sum of squares	F value	P value
Model	352.74	9	39.19	102.48	<0.0001
X_1	9.44	1	9.44	24.68	0.0016
X_2	5.41	1	5.41	14.15	0.0071
X_3	31.01	1	31.01	81.07	<0.0001
X_1X_2	78.89	1	78.89	206.26	<0.0001
X_1X_3	0.017	1	0.017	0.045	0.8379
X_2X_3	203.88	1	203.88	533.05	<0.0001
X_1^2	0.20	1	0.20	0.52	0.4951
X_2^2	7.95	1	7.95	20.79	0.0026
X_3^2	0.46	1	0.46	1.19	0.3112
Residual	2.68	7	0.38		
Lack of Fit	1.92	3	0.64	3.41	0.1335
Pure Error	0.75	4	0.19		
Cor Total	355.42	16			
	$R^2 = 0.9925$	$R^2_{adj} = 0.9828$	CV = 1.05%		

As shown in Table 2, the results showed that the model was significant ($P < 0.001$), and the mismatch term was not significant. $R^2 = 0.99925$ was close to $R^2_{Adj} = 0.9828$, indicating that the model had a good fit, small experimental error, and could better reflect the relationship between the microcapsule embedding rate and wall to core ratio, homogenization time, and wall to core ratio. Therefore, this model could be used to predict the preparation conditions for microcapsules. As shown in Table 2, the coefficients X_1, X_2, X_3, X_{12}, X_{32}, and X_1X_3 had a significant impact on the experimental results ($P < 0.05$), while other coefficients were not significant ($P > 0.05$). The P-value of the mismatch term was 0.1335, indicating that the lack of fitting in the response surface model was not significant.

The response surface experiment results were optimized using Design Expert software, and the optimal conditions for preparing wheat germ peptide microcapsules were obtained as follows: wall to core ratio of 19.74:1, homogenization time of 9.75, and wall to material ratio of SSOA: SA = 2.95:1. The correction conditions were wall to core ratio of 20:1, homogenization time of 10 min, and wall to material ratio of SSOS: SA = 3:1. Under the optimal enzymatic hydrolysis conditions, the predicted embedding rate of wheat germ peptide microcapsules could reach 65.13%. To verify the feasibility of RSM, validation experiments were conducted. The experimental results show that the microcapsule embedding rate could reach 65.33 ± 0.84%, and the relative error

between predicted and actual values was less than 2%, indicating good model fitting and verifying the applicability of the prediction model.

3.3. Particle size analysis of wall materials and microcapsule samples

Fig. 2 showed the particle size distribution of wall material sodium alginate (SA), starch sodium octenylsuccinate (SSOS), and wheat germ peptide microcapsules. As shown in Fig. 2a, it could be seen that SA had the smallest particle size, while the particle size distribution of microcapsules showed a red shift and a significant increase compared to SA and SSOS. The diameter of microcapsules was generally 1–500 μm, while the thickness of the wall material was mostly 0.5–150 μm (Matsuda et al., 2016). Fig. 2b showed the particle size distribution of the wall material and microcapsules. Among them, 99.72% of the microcapsules had a particle size less than 250 μm, with an average particle size of 100.21 μm. 98.91% of sodium alginate particles had a diameter less than 170 μm, with an average particle size of 70.32 μm. 98.09% of SSOS particles had a diameter less than 170 μm, with an average diameter of 76.25 μm, indicating that the size of microcapsules embedded in the wall material would increase. Sun et al. reported the similar results (Sun et al., 2020). Therefore, wheat germ albumin polypeptide microcapsules embedded with starch sodium octenylsuccinate/sodium alginate-based materials by freeze-drying methods belonged to micron sized microcapsules.

3.4. SEM observation of wall materials and microcapsule samples

Fig. 3a showed the electron microscopy image of SA, which showed that SA was irregularly elliptical or elongated, and its size was uneven. Fig. 3b showed the morphology of SSOS under an electron microscope. It could be observed that SSOS was a spherical shape with uneven size and concave surfaces. As shown in Fig. 3c, the results showed the microstructure of wheat germ peptide microcapsules after freeze-drying under an electron microscope. The microcapsules appeared as sheet-like structures of different sizes under the electron microscope. The wall material SA, SSOS, and core material wheat germ peptides were all in small granular form, so the microcapsules were relatively large in size. This might be due to the cross-linking effect between the wall material SA and SSOS, which embedded the core material inside. After vacuum freeze-drying, the water in the microcapsules sublimates, which also leaded to the microcapsules ultimately becoming sheet-like. Adriana et al. presented similar SEM results of microcapsules (Adriana, Misael, & Liliana, 2023).

3.5. FT-IR analysis of wall materials and microcapsule samples

Fig. 4 showed FT-IR of wall material SA, SSOS, and wheat germ peptide microcapsules. As shown in Fig. 4, the results showed that SA, SSOS, and microcapsules all had absorption peaks in the 3500-3000 cm^{-1} amide A band region, indicating the presence of hydrogen bonding forces between the wall material and microcapsules (Niu et al., 2023). However, the characteristic peak intensity of microcapsules in the amide A band region was higher than that of SA and SSOS, indicating the formation of new hydrogen bonds during crosslinking between them (Pawlak & Mucha, 2003). SA was soluble in neutral solutions, and due to the presence of carboxylic acid groups, SA exhibited antisymmetric stretching vibrations at 1617 cm^{-1} and symmetric stretching peaks at 1413 cm^{-1} (Lawrie et al., 2007). The absorption peaks of SA at 1417 cm^{-1}, 1029 cm^{-1}, 1095 cm^{-1}, and 817 cm^{-1} were respectively related to C-N stretching, C-O stretching, C-O-C stretching, and C-H bending vibration (Pan et al., 2021). The absorption peaks of SSOS at 1641 cm^{-1}, 1159 cm^{-1}, 1083 cm^{-1}, 1018 cm^{-1}, and 929 cm^{-1} were all generated by C-O stretching vibration (Chen, Huang, Fu, & Luo, 2014). If the characteristic peaks of wall material SA were basically consistent with those of microcapsules, it proved that the functional groups were not destroyed during the encapsulation process of microcapsules. Compared with the infrared spectrum of peptides, the characteristic peak intensity of microcapsules was significantly weaker, indicating a good embedding effect of microcapsules (Lin, Xu, & Gao, 2024).

3.6. Thermogravimetric analysis of wall materials and microcapsule samples

Thermogravimetric analysis (TGA) is a means of studying the thermodynamics of various samples after thermal degradation, which is used to evaluate the thermal stability of different samples (Sun et al., 2024). When the wall material embeds the core material, the boiling point and melting point of the microcapsules will change accordingly (Guía-García et al., 2023). The TGA curves of microcapsules, SA, SSOS, and wheat germ peptides with a molecular weight less than 3 kDa were shown in Fig. 5. It could be clearly seen that the wheat germ peptides remained in a state of weight loss with heating, which was due to the instability of peptide bioactive substances to heat. The wall materials SA, SSOS, and microcapsules all had two distinct thermal degradation stages. The first weight loss process occurred between 49 and 114 °C, which was due to the weight loss caused by water evaporation (Zhang, 2011). The second weight loss process occurred at 241–253 °C, 296–325 °C, and 278–298 °C, respectively, resulting in an overall weight loss of 64.72%, 79.90%, and 69.786% for the sample. Comparing the thermogravimetric curves of wheat germ peptides and microcapsules, it could be seen that as the pyrolysis temperature of microcapsules increased, the residual mass rate also increased, indicating that microcapsules protected the core material from the loss of wheat germ peptides (Walter et al., 2004).

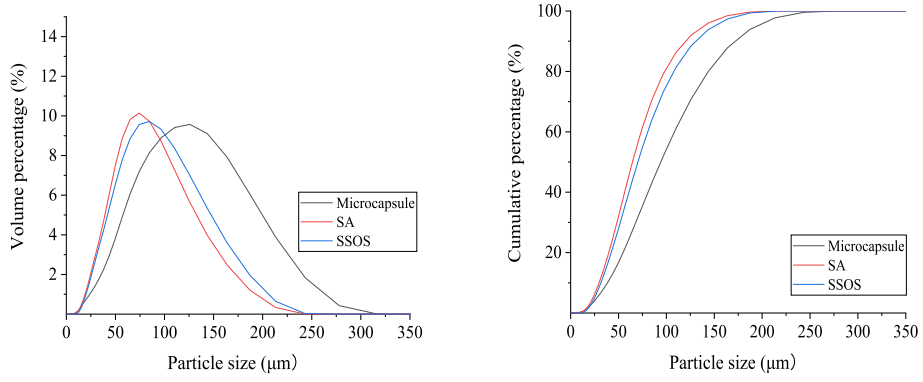

a b

Fig. 2. Particle size analysis of wall materials and microcapsule samples (a: Volume percentage; b: Cumulative percentage).

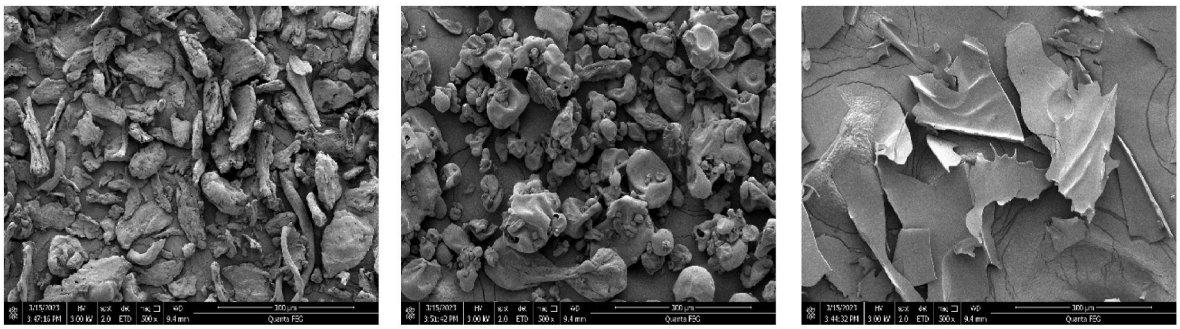

Fig. 3. SEM images of wall materials and microcapsule samples (a: SA 500 × ; b: SSOS 500 × ; c: microcapsule 500 ×).

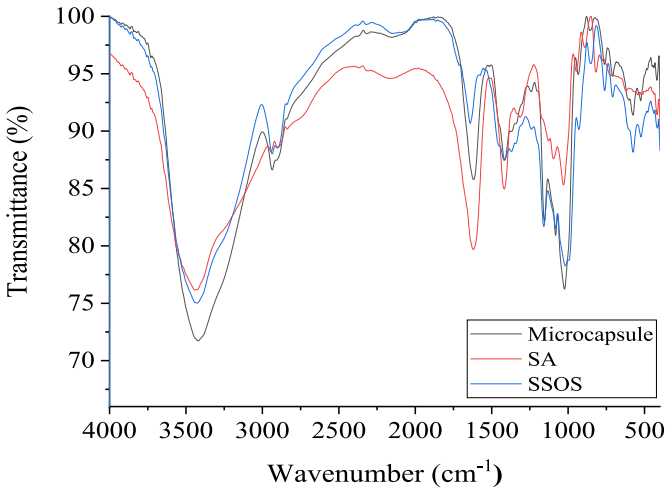

Fig. 4. FT-IR of wall materials and microcapsule samples.

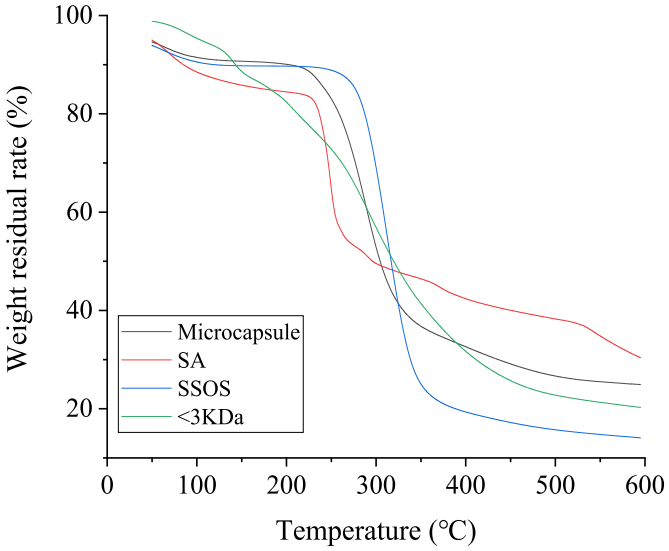

Fig. 5. TGA curve of wall materials and microcapsule samples.

3.7. Sustained-release properties in vitro of wheat germ albumin polypeptides

3.7.1. Artificial simulation of gastric juice digestion experiment

Fig. 6a showed the release rate of wheat germ albumin polypeptide microcapsules in artificial gastric juice. With the prolongation of digestion time, the microcapsules were gradually destroyed in simulated gastric juice, resulting in the release of wheat germ albumin polypeptide microcapsules from the core material.

The wall materials SA and SSOS of the microcapsule were easily soluble in neutral solution, and SA would form hydrogel in acidic gastric juice, which would reduce the solubility of the microcapsule and protect the microcapsule from being digested by gastric juice (Molaveisi & Shi, 2024). However, the freeze-drying wheat germ polypeptide microcapsules were not as tightly embedded as the round microcapsules prepared by spray drying, so part of the microcapsules was destroyed under the digestion of gastric juice (Karthik & Anandharamakrishnan, 2013). After 2 h of artificial simulation of gastric juice digestion, the release rate of microcapsules reached 26.54%, which was lower than the release rate of 30% of astaxanthin microcapsules by Huang et al., using sodium alginate and chitosan (Huang et al., 2024). During the experiment, it was found that solid microcapsules remained after digestion, indicating that microcapsules could stably exist in gastric juice.

3.7.2. Artificial simulation of intestinal juice digestion experiment

Fig. 6b showed the release rate of wheat germ albumin polypeptide microcapsules in artificial intestinal juice, indicating that the release rate of microcapsules in intestinal juice increased with time. The small intestine was the main site for absorbing functional substances, and polypeptides with antioxidant and antihypertensive activities were also targeted for absorption in the small intestine (Li, Shang, Wu, Tan, & Wang, 2024). The release rate of microcapsules in intestinal juice reached 84.41% after 2 h, much higher than the release rate in gastric juice. Due to the ionization of carboxyl groups in sodium alginate in intestinal juice, it increased the electrostatic repulsion between molecules which destroyed the structure of microcapsules, and caused swelling of microcapsules (Lin et al., 2024). In addition, pancreatic enzymes in intestinal juice could destroy proteins and polysaccharides, which could further digest microcapsules (Wani et al., 2023).

In summary, wheat germ albumin polypeptide microcapsules had shown good protective effects, delaying the release rate of wheat germ albumin polypeptides in gastric juice and allowing more bioactive peptides to enter the small intestine targets for absorption, achieving the goal of sustained release.

4. Conclusions

In this study, using the encapsulation rate of microcapsules as an evaluation index, the microencapsulation process conditions of wheat germ albumin polypeptides were optimized. The microcapsules were characterized and conducted *in vitro* simulated digestion experiments. Based on response surface optimization experiments, the optimal process conditions for microencapsulation of wheat germ albumin polypeptides were determined as follows: wall to material ratio SSOS: SA = 3:1, homogenization time 10 min, and wall to core ratio 20:1. The embedding rate of microcapsules prepared under these conditions was

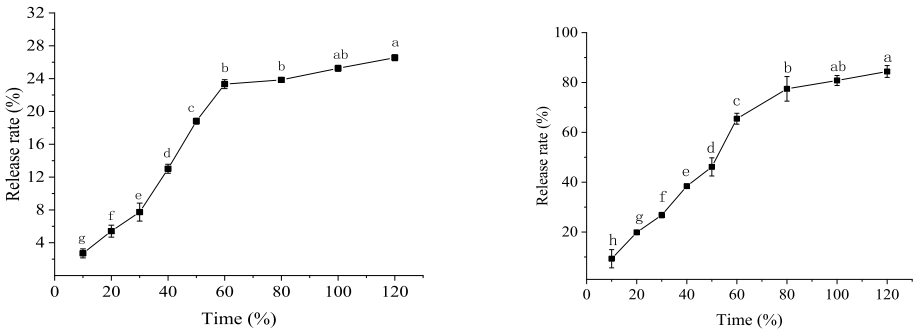

Fig. 6. Sustained-release properties *in vitro* of wheat germ albumin polypeptides (a: Artificial simulation of gastric juice; b: Artificial simulation of intestinal juice).

65.33%. It was found that the average particle size of wheat germ albumin polypeptide microcapsules was 100.21 μm. SEM results showed that the freeze-drying microcapsules had a sheet-like structure. The increased intensity of the amide A band in the microcapsules in Fourier transform infrared spectroscopy indicated the formation of hydrogen bonds between the wall materials, while thermogravimetric analysis confirmed the protective effect of microcapsules on the formation of wheat germ albumin polypeptides. The release rates of microcapsules in gastric and intestinal juice were 26.54% and 84.41%, respectively, indicating that microcapsules had a sustained release effect. Microencapsulation of wheat germ albumin polypeptides can not only protect their biological activity from being destroyed in gastric juice, but also promote small intestine absorption and improve the bioavailability of peptides. Therefore, the transformation of wheat germ resources into new functional and nutritional foods would become a future development trend.

CRediT authorship contribution statement

Shuangqi Tian: Writing – review & editing, Supervision, Funding acquisition, Formal analysis, Conceptualization. **Yuqiu Hu:** Writing – original draft, Investigation, Formal analysis. **Ke Du:** Writing – original draft, Supervision, Investigation. **Jing Lu:** Supervision, Investigation.

Declaration of competing interest

The authors declare that they have no known competing financial interests or personal relationships that could have appeared to influence the work reported in this paper.

Acknowledgements

This research has been funded by the Henan Province International Science and Technology Cooperation Project (242102521003), the Henan Province Key R&D and Promotion Special Project (232102110155), and the Natural Science Innovation Fund Support Program from HAUT (2021ZKCJ12).

Data availability

Data will be made available on request.

References

Abarghoei, M., Goli, M., & Shahi, S. (2023). Investigation of cold atmospheric plasma effects on functional and physicochemical properties of wheat germ protein isolate. *LWT-Food Science and Technology, 177*, Article 114585. https://doi.org/10.1016/j.lwt.2023.114585

Adriana, M., Misael, C., & Liliana, S. (2023). Evaluation of viability, physicochemical properties, and digestibility of freeze-dried *Weissella cibaria* microcapsules during storage. *Food Packaging and Shelf Life, 40*, Article 101164. https://doi.org/10.1016/j.fpsl.2023.101164

Bizzotto, E., Zampieri, G., Treu, L., Filannino, P., Cagno, R. D., & Campanaro, S. (2024). Classification of bioactive peptides: A systematic benchmark of models and encodings. *Computational and Structural Biotechnology Journal, 23*, 2442–2452. https://doi.org/10.1016/j.csbj.2024.05.040

Brandolini, A., & Hidalgo, A. (2012). Wheat germ: Not only a by-product. *International Journal of Food Sciences & Nutrition, 63*, 71–74. https://doi.org/10.3109/09637486.2011.633898

Brestenský, M., Nitrayová, S., Patráš, P., & Heger, J. (2013). Standardized ileal digestibilities of amino acids and nitrogen in rye, barley, soybean meal, malt sprouts, sorghum, wheat germ and broken rice fed to growing pigs. *Animal Feed Science and Technology, 186*(1–2), 120–124. https://doi.org/10.1016/j.anifeedsci.2013.09.006

Chen, H., Huang, Q., Fu, X., & Luo, F. (2014). Ultrasonic effect on the octenyl succinate starch synthesis and substitution patterns in starch granules. *Food Hydrocolloids, 35*, 636–643. https://doi.org/10.1016/j.foodhyd.2013.08.009

Cuomo, F., Cinquanta, C., Trivisonno, M. C., Falasca, L., Greco, M. M., Messia, M. C., et al. (2024). Durum wheat milling by-products for the production of pasta with high nutritional and cooking quality. *LWT-Food Science and Technology, 205*, Article 116504. https://doi.org/10.1016/j.lwt.2024.116504

Do, U. T., Nguyen, Q. T., Kim, J., Luu, Q. S., Park, Y., Song, M., et al. (2024). Tailored synthesis of pH-responsive biodegradable microcapsules incorporating gelatin, alginate, and hyaluronic acid for effective-controlled release. *International Journal of Biological Macromolecules, 270*(Part 1), Article 132178. https://doi.org/10.1016/j.ijbiomac.2024.132178

Gao, C., Jia, J., Yang, Y., Ge, S., Song, X., Yu, J., et al. (2023). Structural change and functional improvement of wheat germ protein promoted by extrusion. *Food Hydrocolloids, 137*, Article 108389. https://doi.org/10.1016/j.foodhyd.2022.108389

Giménez, I., Herrera, M., Escobar, J., Ferruz, E., Lorán, S., Herrera, A., et al. (2013). Distribution of deoxynivalenol and zearalenone in milled germ during wheat milling and analysis of toxin levels in wheat germ and wheat germ oil. *Food Control, 34*(2), 268–273. https://doi.org/10.1016/j.foodcont.2013.04.033

Guía-García, J. L., Charles-Rodríguez, A. V., Silva, P., Robledo-Olivo, A., Cerqueira, M. A., & Flores-López, M. L. (2023). Electrosprayed hydroxypropyl methylcellulose microcapsules containing *Rhus microphylla* fruit extracts and their application in strawberry (*Fragaria* × *ananassa*) preservation. *LWT-Food Science and Technology, 184*, Article 115048. https://doi.org/10.1016/j.lwt.2023.115048

Guo, Q., Chen, P., & Chen, X. (2023). Bioactive peptides derived from fermented foods: Preparation and biological activities. *Journal of Functional Foods, 101*, Article 105422. https://doi.org/10.1016/j.jff.2023.105422

Hosseini, S., Kadivar, M., Shekarchizadeh, H., Abaee, M. S., Alsharif, M. A., & Karevan, M. (2022). Cold plasma treatment to prepare active polylactic acid/ethyl cellulose film using wheat germ peptides and chitosan. *International Journal of Biological Macromolecules, 223*(Part A), 1420–1431. https://doi.org/10.1016/j.ijbiomac.2022.11.112

Huang, J., Zhang, S., Liu, D., Feng, X., Wang, Q., An, S., et al. (2024). Preparation and characterization of astaxanthin-loaded microcapsules stabilized by lecithin-chitosan-alginate interfaces with layer-by-layer assembly method. *International Journal of Biological Macromolecules, 268*(1), Article 131909. https://doi.org/10.1016/j.ijbiomac.2024.131909

Ji, X., He, Y., Xiao, Y., Liang, Y., Yang, W., Xiong, L., et al. (2024). Distribution and safety evaluation of deoxynivalenol and its derivatives throughout the wheat product processing chain. *Food Research International, 192*, Article 114784. https://doi.org/10.1016/j.foodres.2024.114784

Jiang, W., Zhou, G., Wang, C., Xue, Y., & Niu, C. (2021). Synthesis and self-healing properties of composite microcapsule based on sodium alginate/melamine-phenol–formaldehyde resin. *Construction and Building Materials, 271*, Article 121541. https://doi.org/10.1016/j.conbuildmat.2020.121541

Karami, Z., Peighambardoust, S. H., Hesari, J., Akbari-Adergani, B., & Andreu, D. (2019). Antioxidant, anticancer and ACE-inhibitory activities of bioactive peptides from wheat germ protein hydrolysates. *Food Bioscience, 32*, Article 100450. https://doi.org/10.1016/j.fbio.2019.100450

Karthik, P., & Anandharamakrishnan, C. (2013). Microencapsulation of docosahexaenoic acid by spray-freeze-drying method and comparison of its stability with spray-drying

and freeze-drying methods. *Food and Bioprocess Technology, 6*, 2780–2790. https://doi.org/10.1007/s11947-012-1024-1

Kettlewell, P., Byrne, R., & Jeffery, S. (2023). Wheat area expansion into northern higher latitudes and global food security. *Agriculture, Ecosystems & Environment, 351*, Article 108499. https://doi.org/10.1016/j.agee.2023.108499

Lai, C., Hu, L., Tu, J., Li, M., Cui, Q., & Wu, L. (2021). Effects of different alcohol and ultrasonic treatments on thermal and structural properties of zein-starch sodium octenyl succinate composite nanoparticles. *Journal of Food Science, 86*(8), 3574–3588. https://doi.org/10.1111/1750-3841.15845

Lawrie, G., Keen, I., Drew, B., Chandler-Temple, A., Rintoul, L., Fredericks, P., et al. (2007). Interactions between alginate and chitosan biopolymers characterized using FTIR and XPS. *Biomacromolecules, 8*(8), 2533–2541. https://doi.org/10.1021/bm070014y

Li, H., Shang, W., Wu, S., Tan, M., & Wang, H. (2024). Development of intestine-targeted microcapsules for enhanced delivery of fucoxanthin: A strategy to mitigate lipid accumulation *in vitro* and *in vivo*. *Food Bioscience, 59*, Article 104167. https://doi.org/10.1016/j.fbio.2024.104167

Li, J., Shin, G. H., Lee, I. W., Chen, X., & Park, H. J. (2016). Soluble starch formulated nanocomposite increases water solubility and stability of curcumin. *Food Hydrocolloids, 56*, 41–49. https://doi.org/10.1016/j.foodhyd.2015.11.024

Lin, Y., Xu, J., & Gao, X. (2024). Development of antioxidant sodium alginate gel beads encapsulating curcumin/gum Arabic/gelatin microcapsules. *Food Hydrocolloids, 152*, Article 109901. https://doi.org/10.1016/j.foodhyd.2024.109901

Liu, F., Chen, Z., Wang, L., & Wang, R. (2013). Effects of protein solubilisation and precipitation pH values on the functional properties of defatted wheat germ protein isolates. *International Journal of Food Science and Technology, 48*(7), 1490–1497. https://doi.org/10.1111/ijfs.12117

Liu, Y., Guan, L., Meng, N., Wang, L., Liu, M., & Tan, B. (2021). Evaluation of quality deterioration of dried whole-wheat noodles with extrusion-stabilized bran and germ during storage. *Journal of Cereal Science, 97*, Article 103143. https://doi.org/10.1016/j.jcs.2020.103143

Liu, J., Zhang, Y., Liu, J., Zhang, H., Gong, L., Li, Z., et al. (2024). Effect of non-covalently bound polyphenols on the structural and functional properties of wheat germ protein. *Food Hydrocolloids, 149*, Article 109534. https://doi.org/10.1016/j.foodhyd.2023.109534

Mao, Z., Jiang, H., Sun, J., Zhao, Y., Gao, X., & Mao, X. (2024). Research progress in the preparation and structure-activity relationship of bioactive peptides derived from aquatic foods. *Trends in Food Science & Technology, 147*, Article 104443. https://doi.org/10.1016/j.tifs.2024.104443

Matsuda, T., Jadhav, N., Kashi, K. B., Jensen, M., Suryawanshi, A., & Gelling, V. J. (2016). Self-healing ability and particle size effect of encapsulated cerium nitrate into pH sensitive microcapsules. *Progress in Organic Coatings, 90*, 425–430. https://doi.org/10.1016/j.porgcoat.2015.10.021

Molaveisi, M., & Shi, Q. (2024). Enhancement of oxidative stability of camelina oil via Alyssum homolocarpum seed gum/sodium alginate-based microcapsules loaded with *Echinacea purpurea* (L.) extract. *International Journal of Biological Macromolecules, 279*(2), Article 135214. https://doi.org/10.1016/j.ijbiomac.2024.135214

Niu, W., Wu, L., Gong, W., Kang, X., Zhang, J., Nishinari, K., et al. (2023). Properties of complexes of whey protein isolate fibrils (WPIF) and octenyl succinate starch (OSS) and their applications in emulsion stabilization and custard cream. *Food Hydrocolloids, 142*, Article 108822. https://doi.org/10.1016/j.foodhyd.2023.108822

Olalere, O. A., & Gan, C. (2023). Extractability of defatted wheat germ protein and their functionalities in a deep eutectic solvent (DES)-Microwave extraction approach compared to conventional processing. *Sustainable Chemistry and Pharmacy, 32*, Article 101002. https://doi.org/10.1016/j.scp.2023.101002

Pan, J., Li, Y., Chen, K., Zhang, Y., & Zhang, H. (2021). Enhanced physical and antimicrobial properties of alginate/chitosan composite aerogels based on electrostatic interactions and noncovalent crosslinking. *Carbohydrate Polymers, 266*, Article 118102. https://doi.org/10.1016/j.carbpol.2021.118102.

Pawlak, A., & Mucha, M. (2003). Thermogravimetric and FTIR studies of chitosan blends. *Thermochimica Acta, 396*(1–2), 153–166. https://doi.org/10.1016/S0040-6031(02)00523-3

Plaisancié, P., Claustre, J., Estienne, M., Henry, G., Boutrou, R., Paquet, A., et al. (2013). A novel bioactive peptide from yoghurts modulates expression of the gel-forming MUC2 mucin as well as population of goblet cells and Paneth cells along the small intestine. *The Journal of Nutritional Biochemistry, 24*(1), 213–221. https://doi.org/10.1016/j.jnutbio.2012.05.004

Sun, H., Li, S., Chen, S., Wang, C., Liu, D., & Li, X. (2020). Antibacterial and antioxidant activities of sodium starch octenylsuccinate-based Pickering emulsion films incorporated with cinnamon essential oil. *International Journal of Biological Macromolecules, 159*, 696–703. https://doi.org/10.1016/j.ijbiomac.2020.05.118

Sun, Q., Tan, W., Liu, W., Wei, C., Chen, J., Zhao, Z., et al. (2024). Inhibited the walnut oil oxidation through the microcapsules that consisted of (−)-Epigallocatechin gallate and sodium caseinate. *Food Bioscience, 61*, Article 104601. https://doi.org/10.1016/j.fbio.2024.104601

Tian, S., Du, K., Yan, F., & Li, Y. (2022). Microwave-assisted enzymatic hydrolysis of wheat germ albumin to prepare polypeptides and influence on physical and chemical properties. *Food Chemistry, 374*, Article 131707. https://doi.org/10.1016/j.foodchem.2021.131707

Tian, S., Meng, F., Du, K., & Chen, Y. (2023). Biological activity evaluation and identification of different molecular weight peptides from wheat germ albumin. *LWT-Food Science and Technology, 189*, Article 115556. https://doi.org/10.1016/j.lwt.2023.115556

Tonolo F., Fiorese F., Rilievo G., Grinzato A., Latifidoost Z., Nikdasti A., Cecconello A., Cencini A., Folda A., Arrigoni G., Marin O., Pia M.R., Magro M., Vianello F. (2025). Bioactive peptides from food waste: New innovative bio-nanocomplexes to enhance cellular uptake and biological effects. Food Chemistry, 463, 3, 141326. https://doi.org/10.1016/j.foodchem.2024.141326.

Walter, F., Schöll, I., Untersmayr, E., Ellinger, A., Boltz-Nitulescu, G., Scheiner, O., et al. (2004). Functionalisation of allergen-loaded microspheres with wheat germ agglutinin for targeting enterocytes. *Biochemical and Biophysical Research Communications, 315*(2), 281–287. https://doi.org/10.1016/j.bbrc.2004.01.057

Wang, L., Li, T., Sun, D., Tang, M., Sun, Z., Chen, L., et al. (2019). Effect of electron beam irradiation on the functional properties and antioxidant activity of wheat germ protein hydrolysates. *Innovative Food Science & Emerging Technologies, 54*, 192–199. https://doi.org/10.1016/j.ifset.2018.09.003

Wang, Y., Liu, B., Wen, X., Li, M., Wang, K., & Ni, Y. (2017). Quality analysis and microencapsulation of chili seed oil by spray drying with starch sodium octenylsuccinate and maltodextrin. *Powder Technology, 312*, 294–298. https://doi.org/10.1016/j.powtec.2017.02.060

Wani, S. U. D., Ali, M., Mehdi, S., Masoodi, M. H., Zargar, M. I., & Shakeel, F. (2023). A review on chitosan and alginate-based microcapsules: Mechanism and applications in drug delivery systems. *International Journal of Biological Macromolecules, 248*, Article 125875. https://doi.org/10.1016/j.ijbiomac.2023.125875

Wu, B., Cheng, H., Li, X., Yang, Q., Zhang, W., Hao, S., & Wang, C. (2024). Phycocyanin-derived bioactive peptide PCP3 ameliorates lipopolysaccharide-induced small intestinal inflammation in murine intestinal organoids and mice through regulating Akt and AMPK/autophagy signaling. *Food Bioscience, 60*, Article 104419. https://doi.org/10.1016/j.fbio.2024.104419.

Xiao, W., Shen, M., Li, J., Li, Y., Qi, X., Rong, L., et al. (2023). Preparation and characterization of curcumin-loaded debranched starch/Mesona chinensis polysaccharide microcapsules: Loading levels and *in vitro* release. *Food Hydrocolloids, 141*, Article 108697. https://doi.org/10.1016/j.foodhyd.2023.108697

Xun, X., Zhang, Z., Yuan, Z., Tuhong, K., Yan, C., Zhan, Y., et al. (2023). Novel caffeic acid grafted chitosan-sodium alginate microcapsules generated by microfluidic technique for the encapsulation of bioactive peptides from silkworm pupae. *Sustainable Chemistry and Pharmacy, 32*, Article 100974. https://doi.org/10.1016/j.scp.2023.100974

Zhang, B. (2011). Effects of moisture evaporation (weight loss) on fracture properties of high performance concrete subjected to high temperatures. *Fire Safety Journal, 46*(8), 543–549. https://doi.org/10.1016/j.firesaf.2011.07.010

Zhang, Z., Cheng, W., Li, X., Wang, X., Yang, F., Xiao, J., et al. (2023). Extraction, bioactive function and application of wheat germ protein/peptides: A review. *Current Research in Food Science, 6*, Article 100512. https://doi.org/10.1016/j.crfs.2023.100512

Zhang, Y., Wang, Z., Liu, J., Liu, H., Li, Z., & Liu, J. (2024). Interactions of different polyphenols with wheat germ albumin and globulin: Alterations in the conformation and emulsification properties of proteins. *Food Chemistry, 457*, Article 140129. https://doi.org/10.1016/j.foodchem.2024.140129

Zheng, H., Choi, J., Seong, G., & Chung, S. (2020). Preparation, characterization and health benefit functions of unripe apple polyphenols-chitooligosaccharides microcapsule. *Transactions of the Chinese Society of Agricultural Engineering, 36*(14), 281–289. https://doi.org/10.11975/j.issn.1002-6819.2020.14.034

Zhu, K., Zhou, H., & Qian, H. (2006). Proteins extracted from defatted wheat germ: Nutritional and structural properties. *Cereal Chemistry, 83*(1), 69–75. https://doi.org/10.1094/CC-83-0069

Zhuang, K., Sun, Z., Huang, Y., Lyu, Q., Zhang, W., Chen, X., et al. (2022). Influence of different pretreatments on the quality of wheat bran-germ powder, reconstituted whole wheat flour and Chinese steamed bread. *LWT-Food Science and Technology, 161*, Article 113357. https://doi.org/10.1016/j.lwt.2022.113357